Electrochimica Acta 147 (2014) 726–734

Contents lists available at ScienceDirect

Electrochimica Acta

journal homepage: www.elsevier.com/locate/electacta

ELECTROCHEMICAL BEHAVIOR OF PILLAR[5]ARENE ON GLASSY CARBON ELECTRODE AND ITS INTERACTION WITH Cu^{2+} AND Ag^{+} IONS

V.A. Smolko [a], D.N. Shurpik [b], R.V. Shamagsumova [a], A.V. Porfireva [a], V.G. Evtugyn [c], L.S. Yakimova [b], I.I. Stoikov [b], G.A. Evtugyn [a,*]

[a] Analytical Chemistry Department of Kazan Federal University, Kremlevskaya, 18, 420008 Kazan, Russian Federation
[b] Organic Chemistry Department of Kazan Federal University, Kremlevskaya, 18, 420008 Kazan, Russian Federation
[c] Interdisciplinary Center for Analytical Microscopy of Kazan Federal University, Kremlevskaya, 18, 420008 Kazan, Russian Federation

ARTICLE INFO

Article history:
Received 25 August 2014
Received in revised form 1 October 2014
Accepted 2 October 2014
Available online 8 October 2014

Keywords:
electrochemical sensor
pillar[5]arene
mediated electron transfer
cyclic voltammetry
self-aggregation

ABSTRACT

The electrochemical behavior of pillar[5]arene (P[5]A) and of its reaction products with Ag^{+} and Cu^{2+} ions has been investigated using cyclic voltammetry, optical methods and transmission electron microscopy (TEM). Stepwise oxidation of hydroquinone units of P[5]A molecule is guided by self-assembling and acid-base interactions. From one to three hydroquinone units per P[5]A molecule are oxidized depending on the measurement conditions. The deposition of P[5]A on glassy carbon electrode (GCE) partially blocks the electron transduction. Interfering influence of dissolved oxygen can be partially eliminated by the use of carbon black as immobilization matrix. The reaction of P[5]A with silver ions results in formation of most stable form with three benzoquinone and two hydroquinone units stabilized by quinhydrone-like structure. The Ag nanoparticles formed in the reaction retain electron transduction with the electrode due to involvement of shielding P[5]A molecules. Similar reaction with Cu^{2+} ions does not lead to stable products because of the formation of Cu_2O particles detected by UV spectroscopy and TEM. Possible analytical applications of the materials obtained were proved by electrocatalytic reduction of hydrogen peroxide and mediated oxidation of thiocholine as model systems. In both cases, high sensitivity and wide range of the concentration determined were shown.

1. Introduction

Phenolic compounds are widely used in electroanalytical chemistry as mediators of electron transfer and matrices for immobilization of other redox active species and biomolecules [1,2]. Although some substituted phenols tend to oxidation followed by electrode fouling [3], they can be involved in electron transduction by adsorption on solid electrodes [4–6], substitution of polymeric modifier [7], and involvement in the self-organized layers [8] or carbon paste [9]. The interest to the electrochemistry of phenolic compounds is also related to the model investigations of complex electrode reactions complicated with the H^{+} transfer and competitive chemical steps of oxidation/dimerization [10–12]. Substituted phenols are used as industrial reagents in the production of rubber, dyes, plastics, pharmaceuticals, and cosmetics [13]. Some of them like dopamine or l-DOPA are known as metabolites and neurotransmitters which play significant role in biochemical reactions of living beings [14]. Thus the use of electrochemical methods directed to the application and investigations of novel multifunctional phenolic compounds is important in terms of their usability in electrochemical sensors and biosensors [15,16] and monitoring of industrial wastes in pharmacy and clinical chemistry [17–19] and of the surface waters [20].

P[5]A (1), a representative of [1n]paracyclophanes, was synthesized in 2008 by T. Ogoshi et al. from permethylated derivative obtained in one step from commercially available chemicals [21].

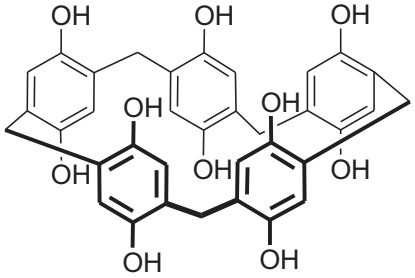

(1)

* Corresponding author. Tel.: +78432337491.
E-mail address: Gennady.Evtugyn@kpfu.ru (G.A. Evtugyn).

http://dx.doi.org/10.1016/j.electacta.2014.10.007
0013-4686/

Its molecule consists of five hydroquinone units linked by methylene bridges. Like cyclodextrines, crown-ethers and calixarenes, P[5]A participates in host-guest complexation with a variety of inorganic and organic cations both in aqueous solutions and organic solvents. In the latter case, its derivatives with long hydrophobic substituents are mainly used to increase solubility and ability to self-aggregation and formation of regular structures on solid supports. The synthesis and host-guest chemistry of P[5]A derivatives was recently summarized in several reviews [22–25]. The interest to P[5]A and its derivatives is initiated by the variety of the structure of the substituents which allows tuning their hot-guest binding properties. In addition, the P[5]A substituted with lipophilic long-chain radicals can self-assemble to form pseudo-rotaxanes [26,27], supramolecular oligomers [28] which are considered as candidates for the artificial transmembrane proton channels [29], fluorescent and UV sensors [30].

Although P[5]A exerts electrochemical activity related to the oxidation of hydroquinone units, the number of publications devoted to its use in electrochemical sensors is rather limited. Thus, the similarity of cyclic voltammograms recorded with P[5]A and hydroquinone in acetonitrile on Pt electrode was mentioned as an evidence of general oxidation mechanism [31]. Permethylated P[5]A was implemented as ionophore in the carbon paste for potentiometric detection of K^+ and Na^+ ions in aqueous solutions [32]. Esterified P[5]A was used in PVC membrane of pH sensitive potentiometric sensor [33].

Hybrid coatings formed by self-assembling of reduced graphene oxide with amphiphilic P[5]A derivative and as-prepared Au nanoparticles were described in [34]. The GCE with hybrid coating exerted electrocatalytic activity and was successfully used for detection of dopamine with low detection limit (12 nM). Contrary to other applications mentioned above, the P[5]A derivative was used in this work for stabilization of suspension of other nanomaterials but not for the electron transduction. Meanwhile the idea to combine P[5]A exerting its intrinsic electrochemical activity with metal nanoparticles seems attractive due to high opportunities of their application in the assembly of electrochemical (bio) sensors.

Previously we have shown the possibility of the chemical synthesis and stabilization of silver nanoparticles by reaction of Ag^+ ions with thiacalix[4]arene bearing catechol fragments in the substituents at the lower rim [35]. The suspension deposited on GCE exerted electrocatalytic effect in dopamine [35] and thiocholine [36] detection. The latter reaction was applied for sensitive determination of cholinesterase inhibitors.

In this work, electrochemical activity of P[5]A and of the products of its interaction with Cu^{2+} and Ag^+ ions was investigated both in solution and on the electrode interface.

2. Materials and methods

2.1. Reagents

Unsubstituted P[5]A was synthesized from 1,4-dimethoxybenzene by removal of protective methoxyl group as described elsewhere [37,38] and schematically represented in scheme (2).

After synthesis, P[5]A was repeatedly rinsed with chloroform and water and then dried. The structure and purity of the product were established by NMR ^1H and MALDI-TOF mass spectroscopy. Product yield: 91%, decomposition without melting at 230 °C. ^1H NMR (d_6-acetone) δ, ppm: 3.66 (10H, s, -CH_2-), 6.64 (10H, s, ArH), 7.99 (10H, s, -OH). MALDI-TOF MS $C_{35}H_{30}O_{10}$: calc. $[M^+]$ m/z = 610.2, found $[M + Na]^+$ m/z = 633.1, $[M + K]^+$ m/z = 649.2.

If not used, P[5]A was stored under Ar at -20 °C. Its solutions in acetone were prepared directly prior to use. If possible, the operations with P[5]A were performed in Ar atmosphere. $AgNO_3$ and $CuSO_4$ (Sigma) were used for preparation of the suspensions of metal nanoparticles.

Thiocholine solutions were prepared by mixing 1.0 mM acetylthiocholine (Sigma) with 10 U mL^{-1} solution of acetylcholinesterase from electric eel (EC 3.1.1.7, 687 U/mg prot.) in 0.1 M phosphate buffer solution in 1:1 v/v ratio. The mixture was incubated for 10 min. to finish the enzymatic hydrolysis of acetylthiocholine.

All other chemicals were of analytical-reagent grade. Aqueous solutions were prepared with Millipore® water.

2.2. Electrochemical measurements

Voltammetric measurements were performed with potentiostat/galvanostat AUTOLAB PGSTAT 302 N (Metrohm Autolab b.v., the Netherlands) at 23 ± 2 °C in the 15 mL working cell. The three-electrode system consisted of working GCE (3.14 mm^2), Ag/AgCl (sat. KCl) reference electrode and Pt wire as a counter electrode. The GCE was mechanically polished by with alumina powder on polishing cloth followed by rinsing with acetone, sulfuric acid and twice with deionized water. Then the electrode was electrochemically cleaned by multiple cycling of the potential between -1.00 and 1.00 V (ten cycles). After cleaning, the electrode was rinsed again with deionized water. The modification of the electrode with P[5]A and its suspension with metal nanoparticles was performed by casting an aliquot of suspension and drying the electrode at ambient temperature.

Coulometric measurements were performed with "Expert-006" analyzer (Econix-Expert, Moscow, Russia) in four-electrode mode with electrogenerated bromine.

2.3. Dynamic light scattering (DLS) and UV-spectroscopy

The metal particle size was determined at ambient temperature by Zetasizer Nano ZS (Malvern) instrument operated with 4 mW He-Ne laser (λ 633 nm) and equipped with noninvasive backscatter optics (NIBS) at the detection angle of 173°. The measurement position in polystyrene cuvette was automatically determined by the software. Absorption spectra were recorded on the UV-3600 UV-spectrometer (Shimadzu) in 10 mm quartz cuvette at 25 °C. The P[5]A (3.0×10^{-5} M) and metal salt (0.1–0.001 M) solutions were prepared in aqueous acetone and dimethylsulfoxide (DMSO) for Ag and Cu composites, respectively. The experiments were carried out in triplicate for each solution.

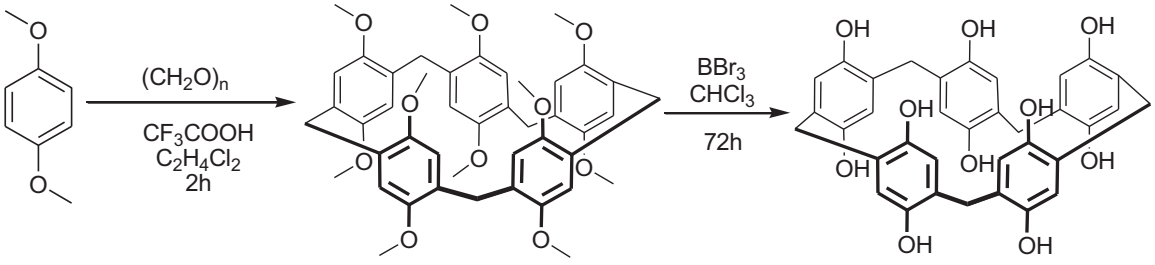

(2)

2.4. Transmission electron microscopy (TEM) measurements

TEM images were obtained with STEM equipped field emission scanning electron microscope Merlin™ (Zeiss, 30 kV, 300 pA) on 400 mesh copper grids coated with Formvar/carbon (Agar Scientific, Cat. No AGS162–4H).

2.5. P[5]A deposition on GCE

Prior to modification, GCE was cleaned as described above and fixed upside down. 2 μL of carbon black (N220, Cabot Corp., Ravenna, Italy) suspension prepared by 30 min. sonication of 1 mg mL^{-1} dispersion in dimethylformamide (DMF) were dispersed on the working area and dried at 70 °C for 20 min. After that, 2 μL of 0.1 mM P [5] solution in acetone were placed on the carbon black layer and the electrode was dried at ambient temperature for 30 min. In some experiments, P[5]A solution was added to DMF dispersion of carbon black prior to its deposition on the electrode.

3. Results and Discussion

3.1. Electrochemical behavior of P[5]A

First, the electrochemical behavior of P[5]A in aqueous organic solvents was investigated on bare GCE. The preliminary estimation of solubility showed that 50% acetone containing 0.1 M Na_2SO_4 was sufficient to solubilize up to 0.01 M P[5]A. The cyclic voltammograms (Fig. 1) contain one pair of semi-reversible peaks at about -110 mV (**1a**) and -420 mV (**1c**). The electron transfer coefficient $\alpha = 0.55$ was calculated from the difference between the oxidation peak potential E_{a1} and the potential of half-peak current $E_{a1/2}$ (3) [39].

$$(1-\alpha)n_\alpha = \frac{47.7mV}{E_{a1} - E_{a1/2}} \quad (3)$$

The peak characteristics correspond to 0.1 mM P[5]A concentration unless otherwise specified. The cathodic peak **1c** is observed in the potential area similar to that of cathodic reduction of dissolved oxygen However, in de-aerated solution the peak increased with the P[5]A concentration so that it corresponds to the reduction of some oxidation products. The peaks **1a** and **1c** are quite stable up to 30 min in repeated recording from the same solution with intermediate stirring. After this period, the cathodic peak **1c** tends to slightly decrease by about 15% of initial value and then stabilizes for the next 60 min (Fig. S1 of Supplementary Materials). The anodic peak **1a** at -110 mV is stable within the whole measurement period and is well reproducible indicating the stability of P[5]A solution in the time interval mentioned. In some experiments in neutral and basic media the anodic peak **1a** has a two-headed shape. Although the peak current is reproducible, the position and resolution of the small heads can differ in consecutive measurements. This might be due to different coordination of the molecules or their associates adsorbed on the electrode.

The second pair of the peaks at 520 (**2a**) and -100 (**2c**) mV appears if the P[5]A concentration exceeds 0.1 mM. Both peaks decreased in a series of repeated records by about 15–20%. This might be related either to partial blocking of the GCE surface or to self-aggregation in solution promoted by oxidation of P[5]A and formation of quinhydrone similar structures with alternating benzoquinone and hydroquinone units of neighboring P[5]A molecules.

The anodic peak current at -110 mV (**1a**) linearly depends on the P[5]A concentration in the range from 10 μM to 0.3 mM in accordance with (4) with the sensitivity of 776 μA mM^{-1} cm^{-2}. This parameter was calculated from the slope of the curve and the square of the electrode surface.

$$I_a,\ \mu A = (0.50 \pm 0.14) + (24.38 \pm 2.33) \times (c, mM),\ R^2 = 0.9725\ (4) \quad (4)$$

The **1a** peak potential insignificantly shifts with P[5]A concentration to less negative values from -140 (10 μM) to -83 (1.0 mM) mV.

The cathodic peak **1c** shows wider linear range of the concentrations from 10 μM to 0.6 mM and sensitivity of 411 μA mM^{-1} cm^{-2} (5).

$$I_c,\ \mu A = (-2.65 \pm 0.84) - (12.92 \pm 3.02) \times (c, mM),\ R^2 = 0.8772\ (5) (5)$$

The peak **2a** observed at high P[5]A concentration is about twofold higher than that of **1a**. Similar ratio was found for cathodic peaks of the pairs mentioned.

Cyclic voltammograms of hydroquinone were recorded for comparison in the same solvent (Fig. 2). Only one pair of the peaks similar to the peaks **1a** and **1c** was found for hydroquinone in the whole range of its concentrations. The anodic peak of P[5]A (**1a**) is shifted against that of hydroquinone to more negative potential and the cathodic peak (**1c**) to less negative potential.

The square of the cathodic peak is significantly higher than that of anodic peak both for hydroquinone and P[5]A. This can be due to

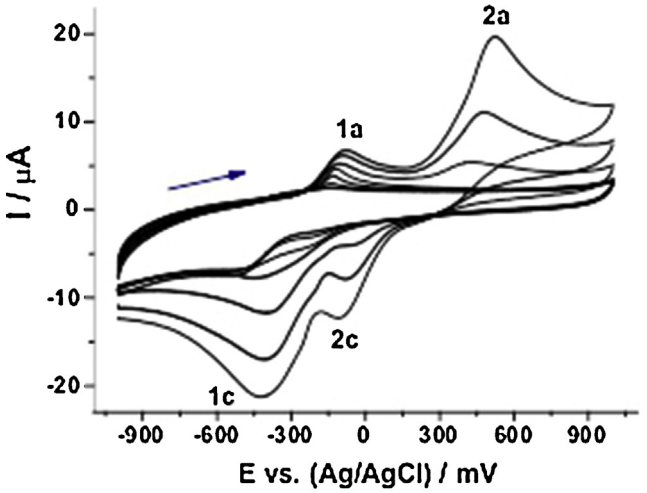

Fig. 1. Cyclic voltammograms recorded on bare GCE in 50% acetone containing 0.1 M Na_2SO_4 in the presence of 10, 30, 60 μM, 0.1, 0.3, 0.6, and 1.0 mM P[5]A at 100 mV s^{-1}, arrow indicates the direction of potential scanning.

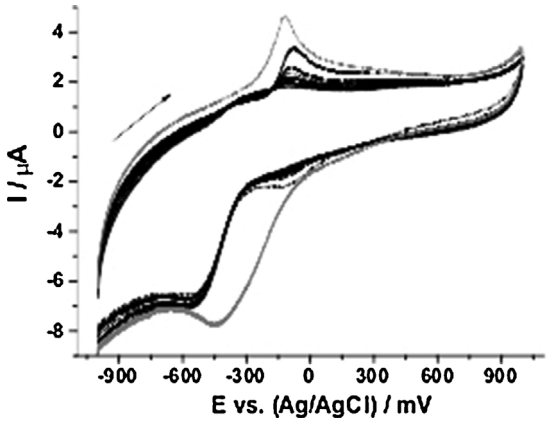

Fig. 2. Cyclic voltammograms recorded on bare GCE in 50% acetone containing 0.1 M Na_2SO_4 in the presence of 20, 40, 60, 80 μM, 0.1, 02, and 0.4 mM hydroquinone (black lines). For comparison, gray line represents the curve of 0.1 mM P[5]A solution; scan rate 100 mV s^{-1}, arrow indicates the direction of potential scanning.

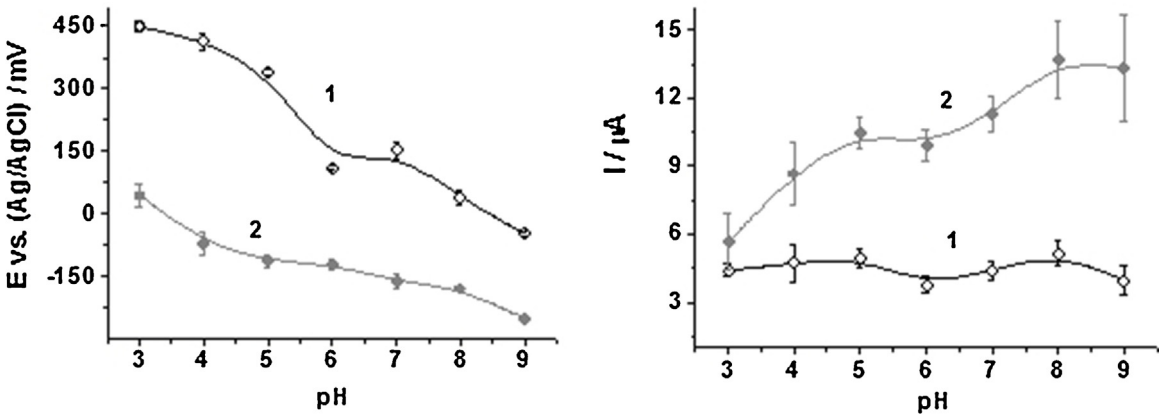

Fig. 3. The dependence of the peak current and peak potential on the pH of working solution. 1–anodic peak **1a**, 2–cathodic peak **1c**. Measurements on GCE in 50% aqueous acetone containing 0.1 M Na_2SO_4 on GCE, scan rate 100 mV s^{-1}. Average values and error bars are calculated for six replications performed with mechanically renewed GCE surface.

adsorption of the oxidation product on the electrode surface. The contribution of adsorption was confirmed by the dependence of the peak current on the scan rate ν. The slope of appropriate dependence in double logarithmic coordinates $(\log I_p)/d(\log \nu)$ was equal to 0.77 for **1a** and 0.67 for **1c**. This indicates mixed surface-diffusion control of the electron transfer. For the peaks **2a** and **2c**, the appropriate values were significantly lower (0.37 and 0.33, respectively).

Coulometric determination of the oxidation stoichiometry performed with electrogenerated bromine in 5% DMSO showed full oxidation of hydroquinone units (10 electrons per one P[5]A molecule). The by-reaction of electrogenerated bromine with the solvent was taken into account in blank experiment. The preparative oxidation of P[5]A with bromine in hexane did not show bromination of aromatic rings or methylene bridges so that all the electrons transferred can be referred to the hydroquinone-benzoquinone conversion.

The pH dependence of the **1a** and **1c** peaks on the voltammogram is asymmetrical (Fig. S2) with the slopes |d*E*p/dpH| equal to 26 and 78 mV for cathodic and anodic peaks, respectively. Formal redox potential E^0 was calculated as a half-sum of the oxidation and reduction peak potentials. Its pH dependence was linear from pH 3.0 to 9.0 with the slope of 60 mV/pH. Assuming two-electron oxidation of the hydroquinone units [40,41], this gives equal number of electrons and hydrogen ions transferred. Higher sensitivity of anodic peak potential toward pH can be due to contribution of intramolecular hydrogen bonds affecting intermediate H^+ transfer and stabilizing anionic phenolate form participating in electron subtraction.(Fig. 3)

Regarding peak current, the cathodic peak regularly increases with pH whereas the anodic peak remains constant within the pH range considered (pH = 4.0–8.0). The divergence of the signals from linear dependencies observed in extreme basic media (pH 9.0) can be referred to competitive oxidation of P[5]A molecules with dissolved oxygen traces present in solution. This coincides with increased deviation of the peak current observed at pH 8.0 and 9.0 against that obtained in neutral and acid solution.

Summarizing the results of investigation of P[5]A solution in aqueous acetone, it is suggested that primary process related to **1a** and **1c** peaks involves oxidation of one hydroquinone unit in P[5]A molecule to benzoquinone. Such a reaction does not disturb the system of hydrogen bonds between neighboring hydroxyl groups of each rim (Fig. 4) which stabilizes the P[5]A spatial structure and its aggregates [42].

Second step (peaks **2a** and **2c**) involves oxidation of two other hydroquinone units. This follows from the relative height of the peaks on voltammogram and is explained by stabilization of the hydroquinone (QH_2) - benzoquinone (BQ) fragment similarly to quinhydrone (QH_2BQ) structure (6). The step of deeper oxidation of P[5]A is observed at rather high concentration of the macrocycle because it can be prevented by association of P[5]A molecules dominating at their low content in solution.

$$(QH_2)_5 \underset{+2e^-,\ +2H^+}{\overset{2e^-,\ 2H}{\rightleftharpoons}} (QH_2)_4(BQ)$$

$$(QH_2)_4(BQ) \underset{+4e^-,\ +4H^+}{\overset{-4e^-,\ -4H^+}{\rightleftharpoons}} \underbrace{(QH_2BQ)_2(BQ)}_{\text{Quinhydrone unit}} \qquad (6)$$

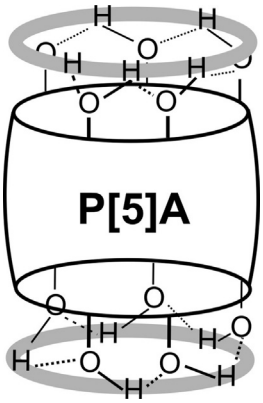

Fig. 4. Layout of cooperative hydrogen bonds at both rims of P[5]A molecule.

The slope of the pH dependency of the formal redox potential (51 mV/pH) calculated for **2a** and **2c** peaks coincides well with the stoichiometry of the hydroquinone oxidation [40,41].

The participation of acid-base equilibria in the reactions of P[5] oxidation was confirmed by titration of P[5]A in 50% aqueous acetone with NaOH. The titration curve contains two steps corresponding to $pKa_1 = 9.5$ and $pKa_2 = 10.7$. The acidity constants

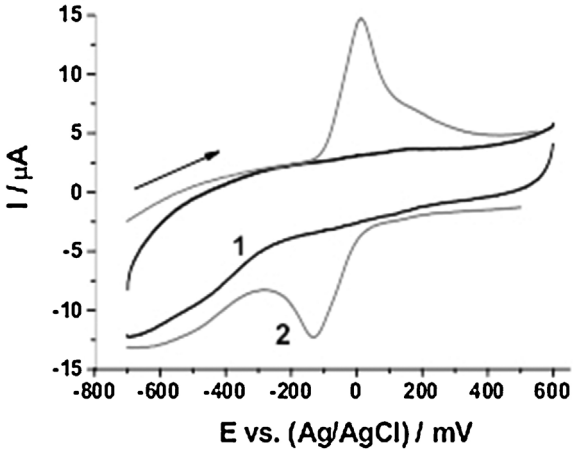

Fig. 5. Cyclic voltammograms recorded on GCE modified (1) with carbon black (1 mg cm^{-2}) and (2) with the same amount of carbon black and 2.0 nanomole P[5]A. Measurements in 0.1 M Na_2SO_4, scan rate 100 mVs^{-1}.

are similar to that of hydroquinone (pKa_1 = 9.85, pKa_2 = 11.4 [43]) and correspond to consecutive formation of two monoanionic zones from both sides of a macrocycle moiety. Thus, from the formal point of view, only one of five hydroquinone units can be ionized in aqueous solution. The mechanism of hydroquinone oxidation in organic solvents with low proton donating properties was determined as *ECE* [44] and it can be accepted for P[5]A oxidation, too.

After the investigations of electrochemical behavior of P[5]A solution in 50% aqueous acetone, the GCE was modified by the macrocycle casted on the working area from anhydrous acetone. The P[5]A film is insoluble in 0.1 M Na_2SO_4 used as supporting electrolyte. Contrary to the experiments with P[5]A solution, it was rather problematic to fully avoid contact of P[5]A placed on the electrode with air so that chemical oxidation of some portion of the macrocycle could take place. Nevertheless, the cyclic voltammograms recorded on modified electrodes were reproducible and coincide with the results obtained with the P[5]A solution (Fig. S3). Maximal changes in the voltammograms were observed for the P[5]A loading of about 0.2 nanomole per electrode. Higher amounts of the P[5]A decrease the currents and their reproducibility in the series of the electrodes because of the formation of irregular thick film visible by naked eye.

In heterogeneous conditions, the second pair of the peaks **2a**,**2c** is much less pronounced than that recorded with P[5]A dissolved in 50% acetone. The peaks **1a** and **1c** are increased with the number of measurements performed on the same electrode with intermediate stirring of the solution. The phenomenon was observed within 60 min. experiment and can be explained by partial dissociation of the aggregates formed on the surface during the modification procedure. The shape of the peaks with a deep current decay after reaching maximum is typical for surface confined processes. The peak **2a** and especially **2c** become relatively smaller against **1a** and **1c** in comparison with previously described experiments in homogeneous solution. This could be also referred to lesser flexibility of association-dissociation processes on the electrode surface.

The pH dependence of the peak potential follows main relationships established for P[5]A solution. The cathodic peak **1c** shifts to more negative values with the slope of 26 mV/pH whereas the anodic peak exerted much higher sensitivity 173 mV/pH. The redox potential E^0 of this peak pair linearly depends on pH in the range from 3.0 to 6.0 with the slope of 83 mV/pH remaining constant in neutral and basic media. Increasing influence of pH on the peak potential in comparison with that observed for P[5]A solution can be due to synergic effect of pH on aggregation and electron transfer observed on the electrode surface.

Although the electrochemical behavior of P[5]A on the electrode surface coincides to that in solution, temporal changes in the peak height and position complicate the quantification of main characteristics of the electrode reactions which were established by renewal of the surface between potential scans. To avoid such complication, several attempts have been made to stabilize the P[5]A in porous conducting matrices. Best results were obtained with carbon black deposited prior to or together with P[5]A on the electrode surface from DMF dispersion. The surface concentration of carbon black was specified before in our previous work on amperometric cholinesterase sensors utilizing thiacalix[4]arene bearing catechol fragments [36].

Fig. 5 shows the cyclic voltammograms recorded on the GCE covered with 1 mg cm^{-2} carbon black and that on the electrode additionally treated with 2.0 nanomole of the macrocycle (2 μL aliquot of 1.0 mM P[5]A solution). One pair of the peak corresponded to **1a**, **1c** peaks of P[5]A was observed. The peak potentials shifted in the presence of carbon black by 150 mV to more negative values due to electrostatic interactions and suppression of P[5]A aggregation on the electrode surface and hence better conditions for electron transfer. What important is that the combination of carbon black and P[5]A made it possible to avoid removal of dissolved oxygen. Measurements in the presence of atmospheric oxygen showed the same peaks as after Ar purging. The peak characteristics did not alter in multiple potential scanning for about 60 min. The electrochemical characteristics of modified electrode remained constant for more than one month storage in dry conditions.

3.2. Interaction of P[5]A with Ag^+ and Cu^{2+} ions

The P[5]A was applied as chemical reducer in reaction with Ag(I) and Cu(II) cations to produce stabilized suspensions of appropriate nanoparticles and then test them in the assembly of the surface layer. The reaction was performed in dark at ambient temperature and monitored electrochemically, by DLS, UV spectroscopy and TEM. The incubation time was varied from 5 to 30 min. but as was shown by the above mentioned methods, all the changes of the properties of reaction mixture finished to 10th - 15th minute depending on the concentration of reactants.

The absorption spectra of P[5]A–$AgNO_3$ system were recorded in aqueous 97% acetone with different amounts of reactants (Fig. S4). A broad band at 350–500 nm with the maximum at 420 nm was observed for 1:1 P[5]A/Ag molar ratio. It can be attributed to the surface plasmon resonance of the silver nanoparticles obtained in chemical reduction of Ag^+ ions by P[5]A molecules [45]. If the quantity of $AgNO_3$ was significantly lower than that corresponded to the stoichiometry ratio (P[5]A:Ag = 10:1), no evidences of nanoparticle formation were found. A broad spectral width and asymmetry of the band can be due to non-ideal crystal structure of Ag particles, specifically due to their non-spherical shape [46], and because of the influence of electromagnetic interactions between neighboring Ag nanocrystals [47]. For 10-fold excess of Ag^+ ions, the plasmon resonance was lower because of the particle aggregation.

The formation of P[5]A stabilized silver nanoparticles was confirmed by DLS data obtained in the same conditions. The systems consisting of the P[5]A and $AgNO_3$ (10:1 and 1:10 mol. eq.) form aggregates with high polydispersity index (PDI) and do not show self-association abilities. Contrary to that, the system P[5]A - $AgNO_3$ (1:1 mol. eq.) provides nanoscale aggregates with the hydrodynamic diameter of 143 ± 12 nm and PDI = 0.19 ± 0.04 (Fig. S5). The hydrodynamic diameter obtained in such dispersion

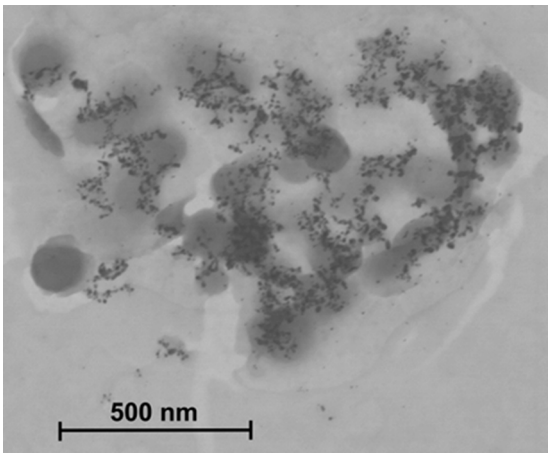

Fig. 6. TEM image of the suspension formed by 0.125 mM P[5]A solution in 95% acetone and 5.0 mM $AgNO_3$ in water, incubation 10 min.

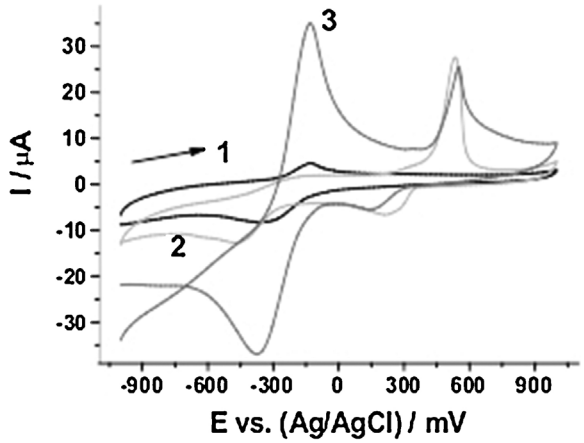

Fig. 7. Cyclic voltammograms recorded on GCE in 0.1 mM P[5]A (1), 1.0 mM $AgNO_3$ (2) and its mixture (3) in 0.1 M Na_2SO_4, pH = 6.5.

assumes aggregation of silver nanoparticles decorated with P[5]A molecules. This was confirmed by TEM (Fig. 6). The ball shaped particles of 15–25 nm are implemented in a less contrast branched structure probably built of P[5]A aggregates. The difference in linear size of the particles determined by both methods is explained by different measurement conditions. In DLS, the hydrodynamic diameter involves the hydrate sphere of the particles and corresponds to the aggregates formed in solution at ambient temperature. TEM images are obtained after drying of the suspension followed by dissociation of weakly bonded sub-particles. Then, only metal core size can be determined by this method with appropriate reliability,

The deposition of P[5]A/Ag mixture on the GCE electrode resulted in remarkable increase of the currents against that of pure P[5]A (Fig. 7). The comparison of the peaks recorded in the solutions of reactants and their mixture shows that silver exerts electrocatalytic effect on the semi-reversible oxidation of P[5]A at -300 . . . -50 mV (see Fig. 1 as a reference) and also produces a sharp peak of the oxidation of elemental silver at about 600 mV. The relative current increase was found about 7.8 for 0.1 mM P[5]A and 1.0 mM $AgNO_3$. The shift of the peak of anodic dissolution of silver to more anodic values could be due to shielding its surface by macrocycle molecules and also due to presence of non-conductive P[5]A layer on the electrode surface. The hysteresis of direct and

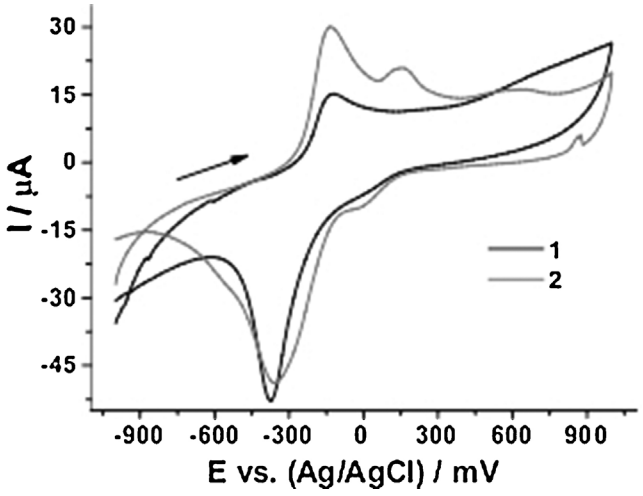

Fig. 8. Cyclic voltammograms recorded on GCE modified with carbon black (1 mg cm^{-2}) in solution of 0.2 mM P[5]A (1) and its mixture with 1.0 mM $CuSO_4$ (2). Measurements in 0.1 M Na_2SO_4, scan rate 100 mV s^{-1}.

reverse branches observed in the first potential scanning at high cathodic potentials can be attributed to the influence of excessive amounts of Ag^+ ions kept in the surface film by electrostatic interactions with carboxylic groups of carbon black. Also, it can be due to non-stationary conditions of the coating caused by slow disaggregation of P[5]A particles. In repeated cycling, the current recorded at high cathodic potentials is significantly decreased and no hysteresis was found to third cycle.

The influence of Ag on P[5]A oxidation increases with their molar ratio with a maximum at Ag: P[5]A = 6:1 corresponding to formation of one benzoquinone and two quinhydrone units $(QH_2BQ)_2BQ$ suggested in scheme (5) for electrochemical oxidation of P[5]A. It should be mentioned that competitive chemical oxidation decreased this ratio in some experiments when initial preparation of P[5]A was stored on air or left in solution for a prolonged period of time. In these conditions the Ag: P[5]A ratio corresponded to the stabilization of the current of Ag oxidation decreased to about 4:1–3:1 so that this parameter can be applied for estimation of the purity of P[5]A preparation. The maximal electrocatalytic effect of Ag depends also on absolute concentration of P[5]A but commonly is reached with $AgNO_3$ concentration of 1.2–1.5 mM. Contrary to that, the maximal anodic current of silver oxidation is observed at much lower concentration of $AgNO_3$ (0.3–0.5 mM) indicating the contribution of silver to aggregation of P[5]A molecules on the electrode surface. Some dependencies of the peak currents related to Ag nanoparticles and P[5]A recorded at different molar ratio of reactants and different P[5]A concentration are given in Supplementary materials (Figs.S6, S7).

Besides casting of the P[5]A/Ag suspension, some experiments were performed with GCE first covered with P[5]A and then soaked in $AgNO_3$ aqueous solution. The resulting voltammogram was similar to that obtained with suspension prepared separately (see Fig. 7). However, the anodic dissolution of Ag was observed only on first scan. The influence of silver on P[5]A own redox activity was also much milder and instable. Lesser effect of Ag^+ can be attributed both to lower amounts of macrocycle involved in reaction and formation of metal nanoparticles with no protective layer of P[5]A molecules.

Similarly to reaction with $AgNO_3$, the same experiments were performed in the mixture of P[5]A and $CuSO_4$. DMSO was used instead of acetone to reach solubility of the copper salt required. The absorbance spectra obtained have a broaden low intensive band at 400–600 nm (λ_{max} 460 nm) typical for Cu(I) nanoparticles [48]. The formation of metallic copper nanoparticles would result in adsorption maximum in the area of 560 nm (Fig. S8). Thus the reaction involves one-electron reduction of Cu^{2+} ions and formation of

insoluble Cu(I) oxide. The complicated chemical step decreases the reproducibility of the voltammograms especially in the area of potentials related to $Cu^{+/2+}$ transfer. The DLS method indicated the high variety of the particle size between 10 and 104 nm and high PDI index. The formation of Cu_2O particles implemented in the hierarchic organic matrix was confirmed by TEM (Fig. S9).

The influence of copper on the P[5]A oxidation was also much lesser than that of silver. Maximal current increase of P[5]A peaks did not exceed 80% for the P[5]A/Cu molar ratio of 1: 10. To improve the reproducibility of the signal, the GCE covered with carbon black was used. An example of cyclic voltammograms recorded in such an electrode is shown in Fig. 8. The peaks related to $Cu^{+/2+}$ transfer are positioned closely to main pair of P[5]A peaks at about 40 mV. The influence of Cu_2O nanoparticles resulted in 60% increase of the P[5]A oxidation current. Meanwhile the reduction current at -350 mV remains constant. Thus the efficiency of electron exchange within the surface layer is too low to significantly improve sensitivity of electrochemical response. Although the influence of Cu^{2+} ions on P[5]A electrochemistry started at very low concentration of about 1.0 nM, its applicability for electroanalysis is rather limited.

3.3. Application to electrochemical sensors

The reversible electrochemical behavior of P[5]A and its aggregates with silver and Cu(I) oxide exerted in a wide range of concentrations can find application in electrochemical sensors and biosensors based on detection of redox active species. As was mentioned above, direct adsorption of P[5]A on the GCE does not allow registration of stable repeatable voltammetric signal probably due to influence of aggregation and pH-dependent equilibria of association-dissociation which alter the redox activity of a modifier. Carbon black was found more appropriate for immobilization of P[5]A and P[5]A/Ag composite. As a proof of applicability of the approach, the determination of hydrogen peroxide and thiocholine was demonstrated in aqueous solution.

Hydrogen peroxide is one of the most common products of enzymatic reactions broadly used for the detection of the substrates of oxidureductases [49]. Direct H_2O_2 oxidation requires rather high overvoltage and can be complicated by competitive oxidation of sample components or electrode fouling. The reduction of H_2O_2 on the GCE covered with carbon black and P[5]A/Ag composite makes it possible to detect 0.1–10 mM of H_2O_2 by specific changes of the cathodic peak current recorded at -50 mV. The value of the current density obtained for 0.1 mM H_2O_2 concentration was found to be 1.33 mA cm^{-2}. This is comparable with that reported for GCE coated with Prussian Blue [50]. The H_2O_2 detection can be performed in the pH region from 3.0 to 7.0. Each sensor makes it possible to perform up to 10 measurements with no losses of the sensitivity. The following stabilization of the signal and increased sensitivity can be expected after the optimization of the surface layer content and measurement protocol. It should be mentioned than carbon black is well compatible with conventional immobilization techniques [51] so that the electrochemical sensor can be then used as transducer of electrochemical enzyme sensors utilizing various oxidoreductases.

Second example of the possible application of P[5]A/Ag composite involves the detection of thiocholine. This is a product of hydrolysis of artificial substrate of acetylcholinesterase which is widely used for quantification of enzyme activity and determination of acetylcholinesterase inhibitors [52–54]. The common reaction used in electrochemical acetylcholinesterase sensors involves mediated oxidation of thiocholine to disulfide (7)

The use of mediator is required because of high overvoltage of direct oxidation of thiocholine and possible interfering reactions of electrode passivation and sulfone formation. Previously we have shown that the introduction of silver nanoparticles resulted in decrease of the working potential from 350 to 150 mV and electrocatalytic thiocholine oxidation accelerated by formation of Ag-S bond. The GCE covered with carbon black and P[5]A/Ag composite showed similar electrocatalytic activity. Measurements were performed in phosphate buffer solution, pH = 7.8, which provided maximal rate of enzymatic hydrolysis of acetylthiocholine. The reliable signal of thiocholine oxidation was detected at 50 mV in the concentration range from 0.1 to 10 mM. High efficiency of electron mediation can be due to involvement of P[5]A shielding layer in electron transduction. similar process with Au electrode covered with self-assembled monolayer with catechol terminal groups has been recently described [55]. The measurements were performed in chronoamperometric mode on the working electrode polarized at 50 mV with consecutive injection of thiocholine aliquots in the stirred phosphate buffer solution, pH 7.0. The dynamic response is shown in Fig. 9. The current was

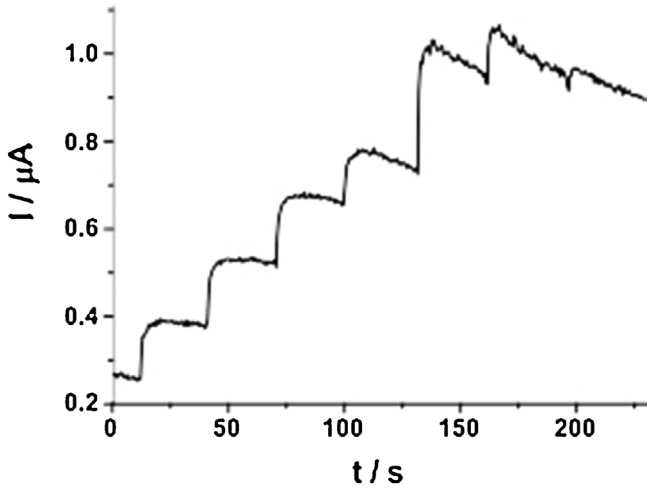

Fig. 9. Dynamic response of the GCE covered with carbon black (1 mg cm^{-2}) and P[5]A/Ag composite toward 0.2, 0.5, 1.0, 1.3, 1.7, 2.0 and 2.5 mM thiocholine at 50 mV. Chronoamperometric regime, 0.1 M phosphate buffer solution, pH 7.8.

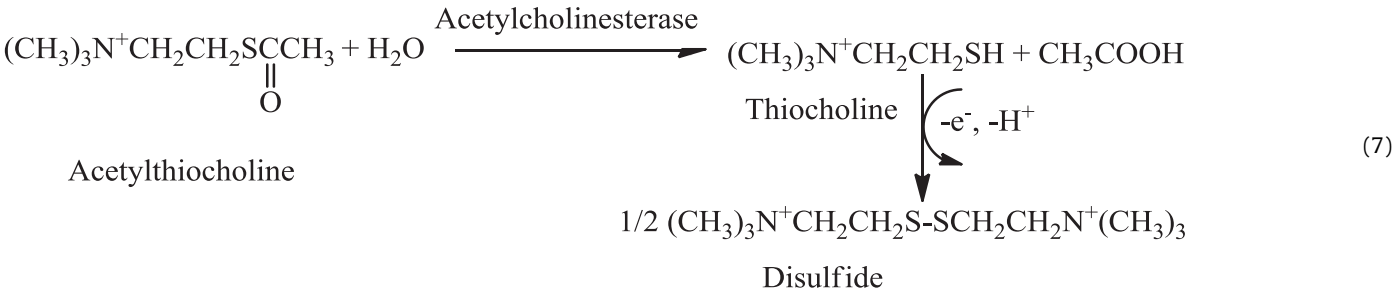

(7)

recorded at maximum reached within 5–7 s after the thiocholine injection. The decrease of the current observed at high thiocholine concentration can be due to passivation of metal nanoparticles caused by chemisorption of by-products or due to deterioration of the surface layer in a long experiment. The following improvement of the stability of the surface layer is the subject of the following experiments.

4. Conclusion

The electrochemical investigation of P[5]A and the products of its reaction with Ag^+ and Cu^{2+} ions showed that the oxidation of hydroquinone units is significantly affected by intramolecular hydrogen bonding and self-aggregation that takes place both in solution and on the electrode surface. At low P[5]A concentration the reaction has mixed surface-diffusion control and results in formation of one benzoquinone unit in the potential area similar to that of monomeric hydroquinone. At high concentration, deeper oxidation takes place with formation of two additional quinhydrone fragments. Thus, 60% efficiency of full P[5]A oxidation observed for chemical oxidants was established by electrochemical methods, either. This might be due to aggregation of the P[5]A molecules followed by partial protection of the rest of hydroxyl groups from oxidation. The stoichiometry of the reaction was confirmed by voltammetric monitoring of the interaction between P[5]A arene and Ag^+ ions resulted in parallel deposition of Ag nanoparticles. Their size, reactivity and redox activity depended on the reactant concentration. The formation of composites including the P[5]A shielding structures and metallic core was confirmed by DLS and TEM. Contrary to that, reaction of P[5]A with Cu^{2+} ions does not lead to stable product. The UV absorbance spectrum evidences in favor of one electron reduction of the copper ions and formation of Cu_2O particles visible on TEM images.

The reversibility of the electrochemical characteristics of P[5]A and P[5]A/Ag composites as well as their stability in the presence of atmospheric oxygen can be significantly improved by deposition on the carbon black layer. The advantages of the future applications of the materials developed in the assembly of electrochemical (bio) sensors were proved by determination of hydrogen peroxide and thiocholine. In both cases, high sensitivity and wide range of the concentrations determined were reached though the stability of the response and sensor lifetime leave place for further improvement by the optimization of the surface layer content.

Acknowledgments

The financial support of the Russian Science Foundation (grant 14-13-00058) is gratefully acknowledged.

Appendix A. Supplementary data

Supplementary data associated with this article can be found, in the online version, at http://dx.doi.org/10.1016/j.electacta.2014.10.007.

References

[1] E.A. Hillard, F.C. de Abreu, D.C.M. Ferreira, G. Jaouen, M.O.F. Goulart, C. Amatore, Electrochemical parameters and techniques in drug development, with an emphasis on quinones and related compounds, Chem. Commun. (2008) 2612.
[2] B. Piro, S. Reisberg, G. Anquetin, H.-T. Duc, M.-C. Pham, Quinone-based polymers for free and reagentless electrochemical immunosensors: application to proteins, antibodies and pesticides detection, Biosensors 3 (2013) 58.
[3] S. Kobayashia, H. Higashimura, Oxidative polymerization of phenols revisited, Prog.Polym.Sci. 28 (2003) 1015.
[4] B. Wannalerse, T. Tuntulani, B. Tomapatanaget, Synthesis, optical and electrochemical properties of new receptors and sensors containing anthraquinone and benzimidazole units, Talanta 64 (2008) 10619.
[5] Y. Dou, S. Haswell, J. Greenman, J. Wadhawan, Immobilized anthraquinone for redox mediation of horseradish peroxidase for hydrogen peroxide sensing, Electrochem. Commun. 11 (2009) 1976.
[6] J. Haccoun, B. Piro, V. Noël, M.C. Pham, The development of a reagentless lactate biosensor based on a novel conducting polymer, Bioelectrochem. 68 (2006) 218.
[7] Z. Algharaibeh, P.G. Pickup, Charge trapping in poly(1-amino-anthraquinone) films, Electrochim. Acta 93 (2013) 87.
[8] V. Ganesh, R.R. Pandey, B.D. Malhotra, V. Lakshminarayanan, Electrochemical characterization of self-assembled monolayers (SAMs) of thiophenol and aminothiophenols on polycrystalline Au: Effects of potential cycling and mixed SAM formation, J. Electroanal. Chem. 619–620 (2008) 87.
[9] M. Aklilu, M. Tessema, M. Redi-Abshiro, Indirect voltammetric determination of caffeine content in coffee using 1,4-benzoquinone modified carbon paste electrode, Talanta 76 (2008) 742.
[10] T.A. Enache, A.M. Oliveira-Brett, Phenol and para-substituted phenols electrochemical oxidation pathways, J. Electroanal. Chem. 655 (2011) 9.
[11] X. Duan, L. Tian, W. Liu, L. Chang, Study on electrochemical oxidation of 4-chlorophenol on a vitreous carbon electrode using cyclic voltammetry, Electrochim. Acta 94 (2013) 192.
[12] S. Ahmed, M. Ahmad, S.B. Butt, Electrooxidation of chloro, nitro, and amino substituted phenols in aqueous medium and their heterogeneous kinetics, Research on Chemical Intermediates 38 (2012) 705.
[13] J. Michałowicz, W. Duda, Phenols - sources and toxicity, Pol. J. Environ. Stud. 16 (2007) 347.
[14] K. Jackowska, P. Krysinski, New trends in the electrochemical sensing of dopamine, Anal. Bioanal. Chem. 405 (2013) 3753–3771.
[15] L. Murphy, Biosensors and bioelectrochemistry, Current Opinion Chem.Biol. 10 (2006) 177.
[16] A.K. Sarma, P. Vatsyayan, P. Goswami, S.D. Minteer, Recent advances in material science for developing enzyme electrodes, Biosens. Bioelectron. 24 (2009) 2313.
[17] J. Dobes, O. Zitka, J. Sochor, B. Ruttkay-Nedecky, P. Babula, M. Beklova, J. Kynicky, J. Hubalek, B. Klejdus, R. Kizek, V. Adam, Electrochemical tools for determination of phenolic compounds in plants. A review, Int. J. Electrochem. Sci. 8 (2013) 4520.
[18] F. Karim, A.N.M. Fakhruddin, Recent advances in the development of biosensor for phenol: a review, Rev. Environ. Sci. Biotechnol. 11 (2012) 261.
[19] Z.-Q. Liu, Chemical methods to evaluate antioxidant ability, Chem. Rev. 110 (2010) 5675.
[20] D.W. Kolpin, M. Skopec, M.T. Meyer, E.T. Furlong, S.D. Zaugg, Urban contribution of pharmaceuticals and other organic wastewater contaminants to streams during differing flow conditions, Sci. Total Environ. 328 (2004) 119.
[21] T. Ogoshi, S. Kanai, S. Fujunami, T. Yamagishi, Y. Nakamoto, Para-bridged symmetrical pillar[5] arenes: their Lewis acid catalyzed synthesis and host-guest property, Journal of the American Chemical Society 130 (2008) 5022.
[22] T. Ogoshi, Synthesis of novel pillar-shaped cavitands pillar[5] arenes and their application for supramolecular materials., J. Incl. Phenom. Macrocycl. Chem., 72,(2012),247.
[23] M. Xue, Y. Yang, X. Chi, Z. Zhang, F. Huang, Pillararenes, a new class of macrocycles for supramolecular chemistry, Acc. Chem.Res. 45 (2012) 1294.
[24] T. Ogoshi, T. Yamagishi, New synthetic host pillararenes: their synthesis and application to supramolecular materials, Bull. Chem. Soc. Jpn. 86 (2013) 312.
[25] T. Ogoshi, T. Yamagishi, Pillararenes: versatile synthetic receptors for supramolecular chemistry, Eur, J. Org. Chem. (2013) 2961–2975.
[26] C. Li, Q. Xu, J. Li, F. Yao, X. Jia, Complex interactions of pillar[5] arene with paraquats and bis(pyridinium) derivatives, Org. Biomol. Chem. 8 (2010) 1568.
[27] T. Ogoshi, H. Kayama, T. Aoki, T. Yamagishi, R. Ohashi, M. Mizuno, Extension of polyethylene chains by formation of polypseudorotaxane structures with perpentylated pillar[5] arenes, Polym. J. 46 l (2014) 77.
[28] T. Ogoshi, Y. Nishida, T. Yamagishi, Y. Nakamoto, Polypseudorotaxane constructed from pillar[5] arene and viologen polymer, Macromolecules 43 (2010) 3145.
[29] W. Si, L. Chen, X.-B. Hu, G.F. Tang, Z.-X. Chen, J.-L. Hou, Z.-T. Li, Selective artificial transmembrane channels for protons by formation of water wires, Angew. Chem. Int. Ed. 50 (2011) 12564.
[30] H. Zhang, N.L. Strutt, R.S. Stoll, H. Li, Z. Zhu, J.F. Stoddart, Dynamic clicked surfaces based on functionalised pillar[5] arene, Chem. Commun. 47 (2011) 11420.
[31] T. Ogoshi, Y. Hasegawa, T. Aoki, Y. Ishimori, S. Inagi, T. Yamagishi, Reduction of emeraldine base form of polyaniline by pillar[5] arene based on formation of poly(pseudorotaxane) structure, Macromolecules 44 (2011) 7639.
[32] L.E. Dube, B.A. Patel, A. Fagan-Murphy, R.R. Kothur, P.J. Cragg, Detection of clinically important cations by a pillar[5] arene-modified electrochemical sensor, Chem. Sens. 3 (2013) 18.
[33] R. Kothur, J. Hall, B.A. Patel, C.L. Leong, M.G. Boutellec, P.J. Cragg, A low pH sensor from an esterified pillar[5] arene, Chem. Commun. 50 (2014) 852.
[34] J. Zhou, M. Chen, J. Xie, G. Diao, Synergistically enhanced electrochemical response of host-guest recognition based on ternary nanocomposites: reduced graphene oxide-amphiphilic pillar[5] arene-gold nanoparticles, ACS Appl. Mater. Interfaces 5 (2013) 11218.
[35] G.A. Evtugyn, R.V. Shamagsumova, R.R. Sitdikov, I.I. Stoikov, I.S. Antipin, M.V. Ageeva, T. Hianik, Dopamine sensor based on a composite of silver nanoparticles implemented in the electroactive matrix of calixarenes, Electroanalysis 23 (2011) 2281.

[36] G.A. Evtugyn, R.V. Shamagsumova, P.V. Padnya, I.I. Stoikov, I.S. Antipin, Cholinesterase sensor based on glassy carbon electrode modified with Ag nanoparticles decorated with macrocyclic ligands, Talanta 127 (2014) 9.
[37] T. Boinski, A. Szumna, A facile, moisture-insensitive method for synthesis of pillar[5] arenes - the solvent templation by halogen bonds, Tetrahedron 68 (2012) 9419.
[38] T. Ogoshi, T. Aoki, K. Kitajima, S. Fujinami, T. Yamagishi, Y. Nakamoto, Facile, rapid, and high-yield synthesis of pillar[5] arene from commercially available reagents and its X-ray crystal structure, J. Org. Chem. 76 (2011) 328.
[39] A.J. Bard, L.R. Faulkner, Electrochemical Methods, Fundamentals and Applications, J. Willey & Sons, New York, 1980.
[40] M.M. Walczak, D.A. Dryer, D.D. Jacobson, M.G. Foss, N.T. Flynn, pH-Dependent redox couple: illustrating the Nernst equation using cyclic voltammetry, J. Chem. Educ. 74 (1997) 1195.
[41] H. Düssel, Š. Komorsky-Lovrić, F. Scholz, A solid composite pH sensor based on quinhydrone, Electroanalysis 7 (1995) 889.
[42] T. Ogoshi, T. Yamagishi, Pillar[5]- and pillar[6] arene-based supramolecular assemblies built by using their cavity-size-depending host-guest interactions, Chem. Commun. 50 (2014) 4776.
[43] D.D. Perrin, Dissociation Consta of Organic Bases in Aqueous Solution, Butterworths, London, 1965 Supplement 1972.
[44] P.D. Astudillo, J. Tiburcio, F.J. González, The role of acids and bases on the electrochemical oxidation of hydroquinone: Hydrogen bonding interactions in acetonitrile, J. Electroanal. Chem. 604 (2007) 57.
[45] M. Ji, X. Chen, C.M. Wai, J.L. Fulton, Synthesizing and dispersing silver nanoparticles in a water-in-supercritical carbon dioxide microemulsion, J. Am. Chem. Soc. 121 (1999) 2631.
[46] V. Klimov, Nanoplasmonics, Pan Stanford Publishing, Singapore, 2014.
[47] M. Quinten, U. Kreibig, Absorption and elastic scattering of light by particle aggregates, Appl. Opt. 32 (1993) 6173.
[48] B.G. Ershov, E. Janata, M. Michaelis, A. Henglein, Reduction of aqueous copper (2+) by carbon dioxide(1-): first steps and the formation of colloidal copper, J. Phys. Chem. 95 (1991) 8996.
[49] A.K. Sarma, P. Vatsyayan, P. Goswami, S.D. Minteer, Recent advances in material science for developing enzyme electrodes, Biosens. Bioelectron. 24 (2009) 2313.
[50] A.V. Borisova, E.E. Karyakina, S. Cosnier, A.A. Karyakin, Current-free deposition of Prussian Blue with organic polymers: towards improved stability and mass production of the advanced hydrogen peroxide transducer, Electroanalysis 21 (2009) 409.
[51] F. Arduini, A. Amine, C. Majorani, F. Di Giorgio, D. De Felicis, F. Cataldo, D. Moscone, G. Palleschi, High performance electrochemical sensor based on modified screen-printed electrodes with cost-effective dispersion of nano-structured carbon black, Electrochem. Commun. 12 (2010) 346.
[52] D. Du, J. Ding, J. Cai, A. Zhang, Electrochemical thiocholine inhibition sensor based on biocatalytic growth of Au nanoparticles using chitosan as template, Sens. Actuators B 127 (2007) 317.
[53] E. Jubete, K. Żelechowska, O.A. Loaiza, P.J. Lamas, E. Ochoteco, K.D. Farmer, K.P. Roberts, J.F. Biernat, Derivatization of SWCNTs with cobalt phthalocyanine residues and applications in screen printed electrodes for electrochemical detection of thiocholine, Electrochim. Acta 56 (2011) 3988.
[54] D. Du, J. Ding, J. Cai, A. Zhang, Electrochemical thiocholine inhibition sensor based on biocatalytic growth of Au nanoparticles using chitosan as template, Sens. Actuators B 127 (2007) 317.
[55] Y. Tian, S. Ye, X. Shi, L. Jing, C. Liang, Y. Xian, An electrochemical platform for acetylcholinesterase activity assay and inhibitors screening based on Michael addition reaction between thiocholine and catechol-terminated SAMs, Analyst 136 (2011) 5084.